TIME SCALE OF CRAB CAVITY FAILURES RELEVANT FOR HIGH LUMINOSITY LHC*

K. Sjobak[†], R. Bruce, H. Burkhardt, A. MacPherson, A. Santamaría García,
CERN, Geneva, Switzerland
Regina Kwee-Hinzmann, Royal Holloway, University of London, Surrey, UK

Abstract

A good knowledge of the effects of the crab cavities, required for the baseline High Luminosity LHC (HL-LHC), is needed before the results of the first tests of crab cavity prototypes in the SPS, planned for 2018, will be available. In case of crab cavity failures, we have to make sure that time scales are long enough so that the beams can be cleanly dumped before damage by beam loss occurs. We discuss our present knowledge and modeling of crab cavity induced beam losses, combined with mechanical deformation. We discuss lower limits on the time scales required for safe operation, and possible failure mitigation methods.

INTRODUCTION

In order to reach the target instantaneous luminosity for the HL-LHC baseline design, crab cavities are necessary [1, 2]. There is no prior experience operating such cavities with a high-energy and high current proton beam like that of the HL-LHC, so the same type of devices will be installed for testing at the SPS. Modeling the effect of the cavity during a failure is therefore important in order to plan their installation and operation both at the LHC and the SPS.

This paper describes a model of the phase and voltage seen by the beam during an abrupt shutdown of the cavity input power, and the effect this has on the beam. This is in itself interesting, and is also an important step towards a realistic model for how the cavity will behave during a quench.

CRAB CAVITY MECHANICAL MODEL

In this work, the deformation of the crab cavity is modeled as a single damped harmonic oscillator which is driven by the pressure of the Lorentz force on the inside of the cavity. The deformation then causes a detuning Δf of the RF resonance frequency. This is an approximation; in reality there are several mechanical modes with different frequencies and different couplings to the RF voltage, and different effect of the RF resonance frequency [3].

This model can be described using the ordinary differential equation (ODE)

$$\sigma \, \mathrm{d}^2 x/\mathrm{d}t^2 + k_D \, \mathrm{d}x/\mathrm{d}t + k_R x = k_F V^2(t) , \qquad (1)$$

where $x(t)$ is the displacement of the cavity surface, σ is the mass per area of the cavity surface, and the coefficients k_R, k_D and k_F scale the pressure from the restoring force,

mechanical damping and the Lorentz force respectively, and $V(t)$ is the deflecting voltage. This can be rewritten as

$$\mathrm{d}^2 x/\mathrm{d}t^2 + 2\xi\omega_m \, \mathrm{d}x/\mathrm{d}t + \omega_m^2 x = k_F V^2/\sigma , \qquad (2)$$

where $\omega_m = \sqrt{k_R/\sigma}$ is the mechanical resonance frequency and $\xi = \frac{k_D}{2\sqrt{\sigma k_R}}$ is the dimensionless damping coefficient.

Assuming that the shift of the RF resonance frequency $\Delta f(t)$ is proportional to the displacement x such that $\Delta f = K_m x$, Eq. (2) can be written as

$$\mathrm{d}^2 \Delta f/\mathrm{d}t^2 + 2\xi\omega_m \, \mathrm{d}\Delta f/\mathrm{d}t + \omega_m^2 \Delta f = K_m k_F V^2/\sigma . \quad (3)$$

In static equilibrium, the Lorentz detuning is given as $\Delta f = K_t V^2$, where K_t is the Lorentz detuning coefficient. Combining this with Eq. (3) yields that

$$K_t = K_m k_F/\omega_m^2 \sigma , \qquad (4)$$

and inserting this into the complete Eq. (3) gives an ODE describing the frequency shift

$$\mathrm{d}^2 \Delta f/\mathrm{d}t^2 + 2\xi\omega_m \, \mathrm{d}\Delta f/\mathrm{d}t + \omega_m^2 \Delta f = \omega_m^2 K_t V^2 , \quad (5)$$

which can be solved to find $\Delta f(t)$. Once $\Delta f(t)$ is known, the phase relative to an oscillator at the reference frequency can be calculated as

$$\phi(t) = \int_0^t 2\pi\Delta f(t') \, \mathrm{d}t' + \phi(0) . \qquad (6)$$

It is assumed that the cavities are correctly tuned at the beginning of the run, at high voltage. The offset $\Delta f_0 = K_t V^2(0)$ is therefore always subtracted from $\Delta f(t)$.

Parameter Estimates

The main parameters of this model are ω_m, K_t, ξ, and the function $V(t)$. From simulations and measurements [4], the Lorentz detuning coefficient of a double quarter wave (DQW) crab cavity with a realistic stiffener takes a value of $K_t \approx -200$ Hz/(MV)^2.

Starting from Eq. (1), we can find an expression for ω_m. Further, by comparing the definitions of K_m and K_t, we get the relation $K_m = K_t V^2/x$. Finally, $k_F V^2$ is the field pressure, which can also be calculated [5] as $\left(\mu_0 H^2 - \epsilon_0 E^2\right)/4$, where E and H is the surface electric and magnetic field. At DQW design voltage $V = 3.34$ MV, the maximum displacement is $x = -1.73$ μm, and it occurs in a region with low magnetic field and an electric field of rougly 3/4 [4] of the maximum value $\hat{E} = 37$ MV/m [6]. Further, the mass per area can be estimated from the wall thickness and mass

---

* Research supported by the High Luminosity LHC project.
† kyrre.ness.sjobaek(at)cern.ch

06 Beam Instrumentation, Controls, Feedback and Operational Aspects

T23 Machine Protection
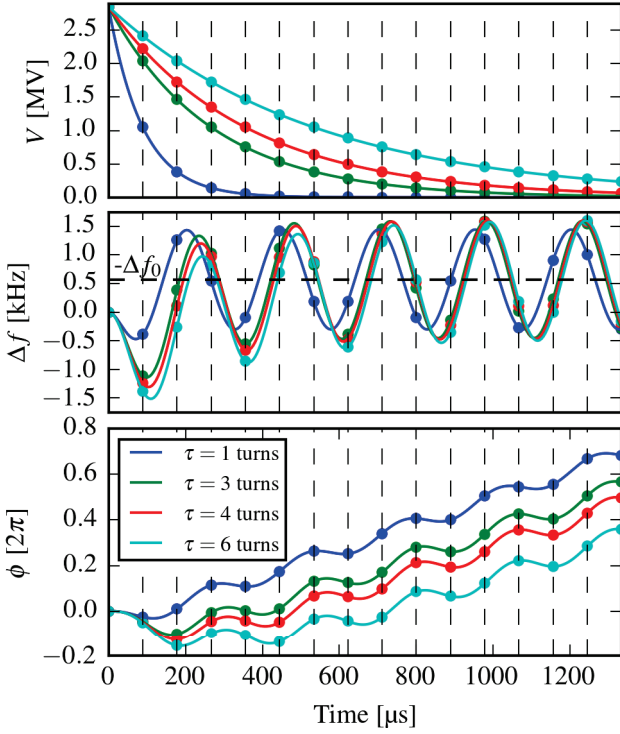
Figure 1: Voltage, RF frequency shift, and phase shift as calculated from Eqs. (5) and (6), with excitation $V(t)$ as given in Eq. (8). The parameter τ is varied, while $f_m = 4000$ Hz, $\xi = 0$ and $V_0 = 2.85$ MV. This high value of the mechanical frequency was selected as it was found in the tracking simulations to produce unusually large losses. The vertical dashed lines indicates the time between LHC turns, and the horizontal line in the Δf plot the equilibrium detuning $-\Delta f_0$ when $V(t) = 0$. The time scale is the same for all the plots. The round markers indicate the values seen by a single bunch passing through the cavity at $t = 0$, t_{turn}, $2t_{turn}$, etc. . . . , as used in the tracking simulations.

density of Niobium, which yields that $\sigma = 32.3$ kg/m^2. Combining these expressions yields an expression for the mechanical frequency

$$\omega_m = \sqrt{\frac{K_m k_F}{K_t \sigma}} = \sqrt{\frac{V^2 k_F}{x \sigma}} = \sqrt{\frac{-\epsilon_0 E^2}{4 x \sigma}}, \qquad (7)$$

which evaluates to $f_m = \omega_m/(2\pi) = 900$ Hz. This approximate estimate of the relevant mechanical resonance frequency indicates that the scale of the frequencies of the interesting eigenmodes is around 1 kHz.

The damping parameter ξ is harder to estimate. However since there are no obvious strong damping effects, it is likely that it is not very large.

The voltage curve $V(t)$ was taken to be

$$V(t) = V_0 \exp(-t/\tau), \qquad (8)$$

where the time constant τ can be estimated as $\tau = 2Q_{ext}/\omega_{RF} = 421$ µs $= 4.73$ LHC turns. This describes
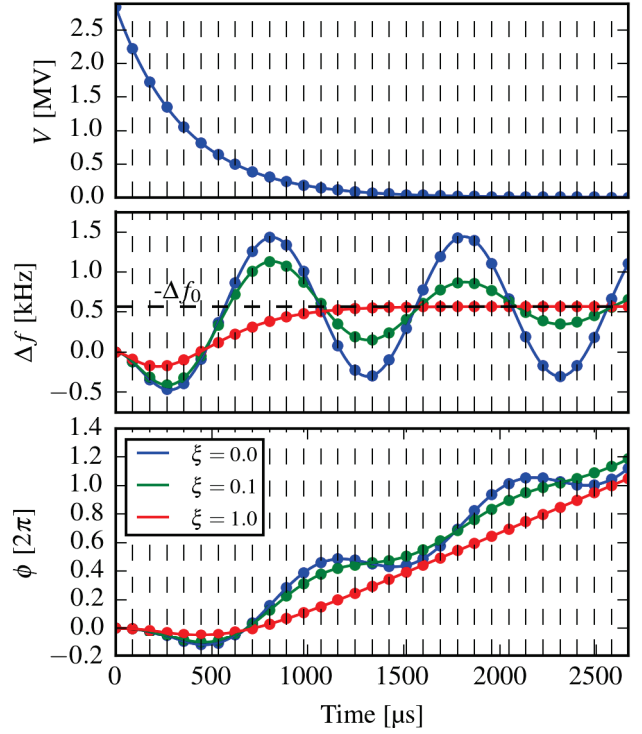
Figure 2: Voltage, RF frequency shift, and phase shift as in Fig. 1. The parameter ξ is varied, while $f_m = 1$ kHz, $\tau = 4$ turns $= 356$ µs and $V_0 = 2.85$ MV. Note that the vertical scale for Δf and ϕ is not the same as in Fig. 1.

the behavior of the cavity voltage in case it stops receiving input power.

Results and Discussion

Some examples of the behavior of the cavities with different voltage decay time scales and damping parameters are shown in Figs. 1 and 2. The initial voltage is here 2.85 MV and not the 3.34 MV discussed earlier, as this is what is needed to compensate for the crossing angle with the HL-LHCv1.2 optics [1].

From Fig. 2, we see that the main effect of the damping parameter is to reduce the initial undershoot of the frequency, at least in the time period where $V(t)$ is still large enough to affect the beam significantly. Regarding the parameter τ from Eq. (8), Fig. 1 shows that it has both an effect on the phase and amplitude of the mechanical oscillation, and on how long $V(t)$ remains significant.

TRACKING SIMULATIONS

In order to quantify the effects on the beam, tracking simulations were ran for the different parameter sets discussed above using the collimation SixTrack version 4.5.34 [7, 8]. With this, 312×64 particles were tracked for each scenario, using the HL-LHC v1.2 optics [1] for Beam 1. The voltage and phase-shift curves discussed above were then applied to all four crab cavities downstream of IP1 using DYNK [9], and the number of particles absorbed in the collimators
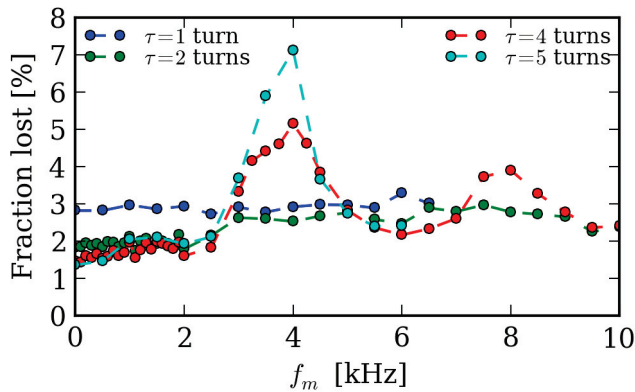
Figure 3: Fraction of beam lost after the onset of failure, as a function of f_m for different voltage fall times τ and $\xi = 0$.

Figure 4: Fraction of beam lost after the onset of failure, as a function of f_m for different ξ and $\tau = 4$ turns.

counted for each turn. The loss was then estimated as the number of particles lost after the onset of the failure, and for normalization the number of particles in the simulation at the onset of the failure was used.

In all cases, the simulation was ran for 40 turns, with the 10 first turns unaffected by the failure in order to clean large-amplitude particles. The simulated beam consisted of one bunch with a Gaussian profile in the transverse phase space. As the amount of losses for $f_m \approx 1$ kHz when using the beam width expected from a nominal normalized emittance of 2.5 μm were negliglible, the transverse width of the beam was increased by a factor 1.8. This distribution is similar to the "tail" part of the double Gaussian distribution discussed in [10, 11], which holds 5% of the beam particles. The longitudinal phase-space distribution of the beam was taken as a multivariate Gaussian, which was then cropped to include only the particles inside of the RF bucket.

Results and Discussion

The tracking results are presented in Figs. 3, 4 and 5. These show that as long as $f_m \lesssim 2$ kHz, the losses are very similar to what is expected from just the voltage drop alone (the 0 Hz points). If the mechanical frequency is further increased, the cavity can respond faster, and at certain frequencies induce quite large losses. As seen in Fig. 3 these losses become more significant for larger τ, as this allows the cavity to affect the beam for a longer time. Finally, it is also seen that when the damping ξ is increased by even a small value, the effect on the beam is noticeably reduced.

The loss positions were checked in a subset of the runs (no detuning and $\tau = 2$ or 4 turns, and $f_m = 4$ kHz and $\tau = 4$ or 5 turns), and virtually all the losses were found to be located in the betatron cleaning insertion (IR7).

The time dependence of the losses for a few characteristic scenarios are shown in Fig. 5. This again shows how the losses normally increase when τ decreases, and how this relationship can be reversed for detuned cavities. Further, it also shows that once the voltage has stopped dropping, a 3-turn pattern in the losses sets in due to the fractional part of the betatron tune, which in the crabbing plane is $Q_y = 60.32$.
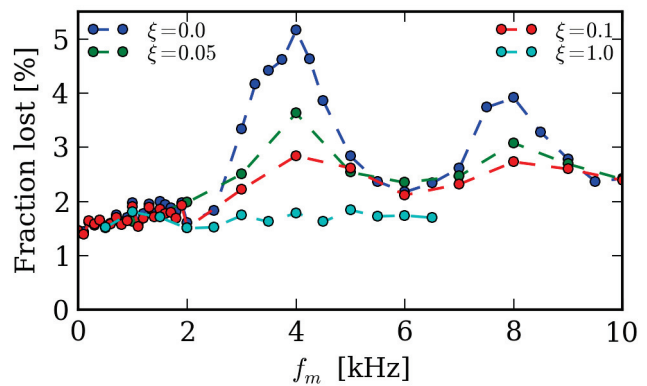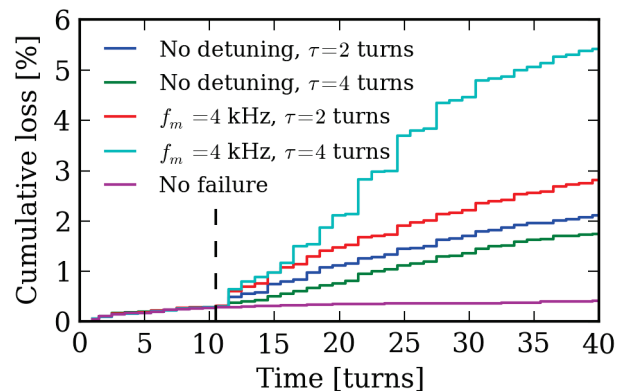
Figure 5: Fraction of beam lost as a function of time for four different similations. In all cases, $\xi = 0.0$. The vertical line indicates the onset of the failure.

Finally, it shows that the losses are gradual and not abrupt. This means that the losses before the beam is dumped, which should happen within 3 turns after the failure is detected, are smaller than what is indicated in Figs. 3 and 4.

CONCLUSIONS AND OUTLOOK

The model presented in this paper combines dynamical Lorentz force detuning with beam dynamics. This showed that for realistic mechanical frequencies, beam losses induced by RF phase change from the mechanical resonances are not expected to exceed the losses caused by simply draining the cavity. However, this depends on the mechanical frequencies staying below approximately 2 kHz.

Some factors which will modify the shape of $V(t)$ are the RF control system, beam loading, and dynamically changing Q-factor during a quench in a superconducting cavity. Further, a real cavity will have multiple resonance modes with different frequencies and ξ. Including these effects is likely to yield further insights and reduce the uncertainities.

REFERENCES

[1] "High-Luminosity Large Hadron Collider (HL-LHC) Technical Design Report V0", EU Deliverable D1-10, https://edms.cern.ch/ui/file/1558149/

[2] Q. Wu, "Crab cavities: Past, present and future of a challenging device", in *Proc. 6th Int. Particle Accelerator Conf. (IPAC'16)*, Richmond, VA, USA, May 2015, paper THXB2, pp. 3643-3648, http://cds.cern.ch/record/2114108/files/CERN-ACC-2015-0189.pdf

[3] J. R. Delayen, "Ponderomotive instabilities and microphonics – a tutoriaL", In *Proc. of the 12th Int. Workshop on RF Superconductivity (SRF'05)*, Cornell University, Ithaca, NY, USA, Jul. 2005, paper SUP01, pp. 35-39, https://accelconf.web.cern.ch/accelconf/SRF2005/papers/sup01.pdf

[4] S. Verdú-Andrés, S.A. Belomestnykh, J. Wang, Q. Wu, and B. P. Xiao, "Lorentz Detuning for a Double-Quarter Wave Cavity", in *Proc. 17th Int. Conf. on RF Superconductivity (SRF'15)*, Whistler, BC, Canada, Sep. 2015, paper THPB051, pp. 1215–1218, doi:10.18429/JACoW-SRF2015-THPB051

[5] E. Haebel and J. Tückmantel, "Electromagnetic surfaces forces in RF cavities", CERN, Geneva, Switzerland, Rep. CERN-AT-RF-INT-91-99, Dec. 1991, http://cds.cern.ch/record/950375/files/CM-P00058119.pdf

[6] S. Verdú-Andrés, L. Alberty, K. Artoos, S.A. Belomestnykh, I. Ben-Zvi, R. Calaga, O. Capatina, T. Capelli, F. Carra, N. Kuder, R. Leuxe, Z. Li, A. Ratti, J. Skaritka, Q. Wu, B. P. Xiao, and C. Zanoni, "Design and prototyping of HL-LHC double quarter wave crab cavities for SPS test", in *Proc. 6th Int. Particle Accelerator Conf. (IPAC'16)*, Richmond, VA, USA, May 2015 paper MOBD2, pp. 64-66, http://jacow.org/IPAC2015/papers/mobd2.pdf

[7] SixTrack, http://sixtrack.web.cern.ch/SixTrack/

[8] G. Robert-Demolaize, R. Assmann, S. Redaelli, and F. Schmidt, "A new version of SixTrack with collimation and aperture interface", In *Proc. 2005 Particle Accelerator Conf. (PAC'05)* , Knoxville, Tennessee, USA, May 2005, paper FRAT081, pp. 4084-4086, http://accelconf.web.cern.ch/accelconf/p05/PAPERS/FPAT081.PDF

[9] K. Sjobak, H. Burkhardt, R. De Maria, A. Mereghetti, and A. Santamaria Garcia, "General functionality for turn-dependent element properties in SixTrack", in *Proc. 6th Int. Particle Accelerator Conference (IPAC'15)*, Richmond, VA, USA, May 2015, http://accelconf.web.cern.ch/AccelConf/IPAC2015/papers/mopje069.pdf

[10] B. Yee-Rendon, R. Lopez-Fernandez, J. Barranco, R. Calaga, A. Marsili, R. Tomás, F. Zimmermann, and F. Bouly, "Simulations of fast crab cavity failures in the high luminosity Large Hadron Collider", *Phys. Rev. ST Accel. Beams*, vol. 17, p. 051001 , May 2014, http://link.aps.org/doi/10.1103/PhysRevSTAB.17.051001

[11] A. Santamaria Garcia, K. Sjobak, R. Bruce, H. Burkhardt, F. Cerutti, R. Kwee-Hinzmann, and A. Lechner, "Machine and experiment protection from fast crab cavity failures in the HL-LHC", presented at the 7th Int. Conf. on Particle Accelerators, Busan, Korea, May 2016, paper , this conference.